

Article

# Hierarchical coculture of hepatocytes, hepatic stellate cells, and sinusoidal endothelial cells for TGF- $\beta$ -induced early liver fibrosis studies in vitro

Qiao You Lau <sup>1,2\*</sup>, Fuad Gandhi Torizal <sup>2,3</sup>, Marie Shinohara <sup>1</sup>, and Yasuyuki Sakai <sup>1,2,3</sup>

<sup>1</sup> Institute of Industrial Science, The University of Tokyo, Tokyo, Japan; QLAU001@e.ntu.edu.sg (Q.Y.L), marie-s@iis.u-tokyo.ac.jp (M.S.), sakaiyasu@chemsys.t.u-tokyo.ac.jp (Y.S.)

<sup>2</sup> Department of Bioengineering, Graduate School of Engineering, The University of Tokyo, Tokyo, Japan; QLAU001@e.ntu.edu.sg (Q.Y.L), t\_gandhi@chemsys.t.u-tokyo.ac.jp (F.G.T), sakaiyasu@chemsys.t.u-tokyo.ac.jp (Y.S.)

<sup>3</sup> Department of Chemical System Engineering, Graduate School of Engineering, The University of Tokyo, Tokyo, Japan; t\_gandhi@chemsys.t.u-tokyo.ac.jp (F.G.T), sakaiyasu@chemsys.t.u-tokyo.ac.jp (Y.S.)

\* Correspondence: QLAU001@e.ntu.edu.sg ; Tel.: +81-5841-7073

**Abstract:** During chronic liver injury, inflammation leads to liver fibrosis— particularly due to the activation of hepatic stellate cells (HSCs). However, the involvement of inflammatory cytokines in HSC activation and the relationship between each type of liver cells is still unclear. To examine their interactions, many existing in vitro liver models were performed in 3D organoid or spheroid culture with random 3D structure, which complicates analysis. Herein, we demonstrated the hierarchical coculture of primary rat hepatocytes with non-parenchymal cells such as the human-derived HSC line (LX-2) and the human-derived liver sinusoidal endothelial cell line (TMNK-1). The cocultured tissue had high usability with simple operation of separating solid and liquid phases with improved liver functions such as albumin production and hepatic cytochrome P450 3A4 activity. We also studied the effects of stimulation by both oxygen tension and the key pro-fibrogenic cytokine, transforming growth factor beta (TGF- $\beta$ ), on HSC activation. Gene expression analysis revealed that lower oxygen tension and TGF- $\beta$ 1 stimulation enhanced collagen type I and alpha-smooth muscle actin expression from LX-2 cells in the hierarchical coculture after TGF- $\beta$ 1 stimulation. Therefore, this hierarchical in vitro cocultured liver tissue could provide an improved platform as a disease model for elucidating the interactions of various liver cell types and biochemical signals in future liver fibrogenesis studies.

**Keywords:** fibrogenesis; hepatic stellate cells; coculture; transforming growth factor beta; oxygen tension

## 1. Introduction

Liver fibrosis is a common pathological outcome of several chronic liver diseases, such as viral hepatitis, and results from extracellular matrix (ECM) accumulation following hepatic stellate cell (HSC) activation and proliferation [1], which gives them pro-inflammatory and fibrogenic properties [2]. Despite the high prevalence and detrimental outcomes, many current treatments are restricted to relieving chronic stresses, and no effective therapies are available [3,4]. Therefore, researchers are challenged to reveal detailed liver fibrosis mechanisms and develop efficient drugs for clinical treatment. Animal testing is still the most common preclinical assessment mode, but sometimes, there is poor prognostic value regarding both efficacy and toxicity in terms of the human physiological response [5,6]. Furthermore, there are many ethical concerns about the use of animal models [5].

Current in vitro liver tissue models for fibrosis studies are often performed in a two-dimensional culture of hepatocyte monoculture or hepatocyte and HSC cocultures [7]. Primary hepatocytes have

been commonly utilized in *in vitro* liver tissue models to evaluate the drug metabolism and toxicity. However, hepatocyte functions are compromised and, therefore, are far from recapitulating liver tissues' functions because of the rapid de-differentiation and short-term survival of *in vitro* cultured hepatocytes, limiting the generation of functional engineered liver tissues [8]. Also, the availability of human hepatocytes for clinical, research, or pharmaceutical applications is low due to the shortage of human organs, driving up the cost. This shortage is exacerbated by the inability to expand primary hepatocytes *in vitro* [9]. For these reasons, most human hepatocytes are isolated from livers rejected for transplantation or marginal (fibrotic, fatty) livers that are not optimal for developing culture models for disease studies [10]. Hence, alternative primary cell sources from animals are usually harvested for functional studies purposes.

As a liver fibrosis model *in vitro*, hypoxia has been considered a stress factor that may lead to the activation of HSCs [11], and HSC monocultures have been evaluated by stimulation with various pro-fibrotic and pro-inflammatory cytokines to enable the investigation of how the inflammation-driven complex microenvironment affects HSC activation and fibrosis development [1,12]. However, the interactions between hepatocytes and HSCs could not be observed in monocultures (e.g., The pro-inflammatory factor secretion from hepatocytes enhances HSC activation, resulting in excess collagen fiber produced by activated HSCs and myofibroblasts, which interferes with hepatic functions). Moreover, other non-parenchymal cells, such as sinusoidal endothelial cells, should be considered. Therefore, the lack of robust and biologically relevant liver fibrosis *in vitro* models for functional pharmacokinetics and toxicological studies poses a significant problem associated with the development of effective therapies [13–15], as many of these models focus only on the parenchymal hepatocytes or non-parenchymal cells (NPCs) [16] while overlooking interactions from the surrounding hepatic cells [17]. Consequently, stable cocultured liver tissue formation for liver fibrosis studies is desired.

The long-term behavior of hepatocytes might be modulated by heterotypic cell-cell interactions in three-dimensional engineered tissues [8], and it is widely known that coculturing with NPCs could improve the microenvironments of cells [18,19], hence assisting in stabilizing the phenotype of hepatocytes [17]. Nonetheless, many difficulties emerge when establishing a functional liver tissue culture system. For instance, three-dimensional cocultures are usually performed in organoid cultures for studying liver diseases such as steatosis [20]. However, the structure of 3D organoids is random, and the interactions between each cell type are not uniform, which makes it challenging to examine the response from various tissues. In other studies, Du et al. reported that hepatocyte, HSC, LSEC, and Kupffer cell coculture in a microfluidic device enhanced hepatic function. Even though they achieved hierarchical structure formation, cell-cell interaction between hepatocytes was lost [21]. Instead, Xiao et al. developed an *in vitro* liver-like tissue coculture system and demonstrated that direct oxygenation through the polydimethylsiloxane (PDMS) membranes permitted the organization of hierarchical multilayer of primary rat hepatocytes and human liver sinusoidal endothelial cell line (TMNK-1). Such culture on PDMS surface could achieve multilayer tissue culture, which could not be achieved in cultures on conventional tissue culture polystyrene that could prove to be useful in comprehensive studies of cell signaling pathways between parenchymal and non-parenchymal cells and the understanding of heterotypic cell-cell interactions critical for functionalities of the liver [17]. Thus, the direct incorporation of NPCs such as HSCs and liver sinusoidal endothelial cells (LSECs) in *in vitro* liver platforms is vital for emulating the functions of the liver to establish a tissue-specific and physiologically relevant model for the study of liver fibrosis, which could lead to efficient novel drug development and a more accurate prediction of the functional and safety drug dosage.

In this study, we aimed to develop an *in vitro* liver tissue to simulate an *in vivo*-like liver tissue physiology by a hierarchical coculture of both the parenchymal rat hepatocytes and NPCs – HSCs and LSECs. We used rat hepatocytes instead of human hepatocytes because rat hepatocytes are stable and can retain their functions when cultured for about two weeks. Also, other cell sources of primary human hepatocytes, such as human iPS cells-derived hepatocytes and chimeric mice hepatocytes, are

---

still under scrutiny. The response of HSCs to activation by varying the physiological parameters, such as oxygen concentration and exposure to the well-known pro-fibrogenic mediator, TGF- $\beta$  [22], were then characterized. We hypothesized that this coculture system would respond to the fibrogenic effects due to these stimulations and could, therefore, be used to study the liver fibrogenesis phenomenon *in vitro*. In the future, this concept could be widely applicable to the coculturing of multiple cell types in microphysiological systems (MPS) for high-throughput screening of various compounds.

## 2. Materials and Methods

### 2.1. Rat hepatocyte isolation

Primary hepatocytes were isolated from 7 to 8-week-old male Wistar rats (Sankyo Laboratory, Japan) by a two-step collagenase perfusion technique [23] and suspended in ice-cold, seeding Williams' E Medium (Gibco, Japan). All animals were treated in accordance with the University of Tokyo guidelines for animal experiments and following the guidelines of the Japanese Ministry of Education.

### 2.2. Hepatocyte monoculture

Isolated primary rat hepatocytes were seeded at a density of  $1.0 \times 10^5$  cells/cm<sup>2</sup> on PDMS plates to form a confluent monolayer on day -3. The Williams' Medium E was supplemented with 0.1  $\mu$ M dexamethasone (Wako, Japan), 10 ng/ml mouse epidermal growth factor (EGF) (Takara, Japan), 0.5 mM ascorbic acid 2-phosphate (Wako, Japan), 1% GlutaMAX-I (Gibco, Japan), 1% Insulin-Transferrin-Selenium (ITS-G) (Gibco, Japan), 15 mM HEPES (STAR Chemical, Japan), and 1% antibiotic and antimycotic solution consisting of penicillin, streptomycin, and amphotericin B (Wako, Japan). Hepatocytes were cultured in a humidified incubator at 37°C in a 10% O<sub>2</sub> and 2.5% O<sub>2</sub> atmosphere up to day 14, with medium replacement performed every other day.

### 2.3. Hepatic non-parenchymal cell culture

LX-2, a human-derived hepatic stellate cell (HSC) line, was maintained in Dulbecco's modified eagle's medium (DMEM) high glucose basal media (Wako, Japan) supplemented with 10% fetal bovine serum (FBS) (Gemini Bio-Products, Japan), 1% GlutaMAX-I (Gibco, Japan), and 1% antibiotic and antimycotic solution consisting of penicillin/streptomycin (P/S) and amphotericin B (Wako, Japan). TMNK-1, a human-derived liver sinusoidal endothelial cell (LSEC) line, was maintained in MCDB 131 medium (Gibco, Japan), supplemented with endothelial cell growth medium-2 singlequots supplements (Lonza, Japan) with the exclusion of GA-1000. This was further supplemented with 1% antibiotic and antimycotic solution consisting of P/S and amphotericin B (Wako, Japan). The respective culture medium was changed every two days, and the cells were passaged at approximately 80% confluency.

### 2.4. Coculturing hepatocytes with hepatic non-parenchymal cells

On day -3, rat hepatocytes were seeded at a density of  $1.0 \times 10^5$  cells/cm<sup>2</sup> to form a confluent monolayer in pretreated 24-well or 96-well polydimethylsiloxane (PDMS) plates (Vessel, Japan), which facilitate direct oxygenation of cells by diffusion through PDMS membranes that could maintain cell viability and function [24] (Figure 1). PDMS surfaces were treated with oxygen plasma for 60 s using the YHS-GZA 200 (SAKIGAKE-Semiconductor, Japan) and coupled with (3-mercaptopropyl)-trimethoxysilane (TCI, Japan). The introduced amino groups were reacted with a cross-linker, *N*-(4-maleimidobutyryloxy)-succinimide (GMBS) (Dojindo, Japan), and subsequently activated by 1-ethyl-3-(3-dimethylaminopropyl)-carbodiimide, hydrochloride (WSC) (Dojindo,

Japan), and N-hydroxysulfosuccinimide sodium salt (sulfo-NHS) (TCI, Japan). Finally, the PDMS surfaces were coated with collagen type I-P (Nitta Gelatin, Japan) to facilitate cell attachment.

On day -2, LX-2 cells were seeded onto rat hepatocytes at a density of  $5.0 \times 10^3$  cells/cm<sup>2</sup>. On day -1, TMNK-1 cells were seeded onto the cocultures at a density of  $1.0 \times 10^5$  cells/cm<sup>2</sup>. The hierarchical cocultures were then cultured for one day. They were cultured in a humidified incubator at 37°C in 5% CO<sub>2</sub> and 20% O<sub>2</sub>. Culture medium was changed every two days with Williams' Medium E containing 0.1 μM dexamethasone (Wako, Japan), 10 ng/ml mouse epidermal growth factor (EGF) (Takara, Japan), 0.5 mM ascorbic acid 2-phosphate (Wako, Japan), 1% GlutaMAX-I (Gibco, Japan), 1% Insulin-Transferrin-Selenium (ITS-G) (Gibco, Japan), 15 mM HEPES (STAR Chemical, Japan), and 1% antibiotic and antimycotic solution consisting of penicillin, streptomycin, and amphotericin B (Wako, Japan).

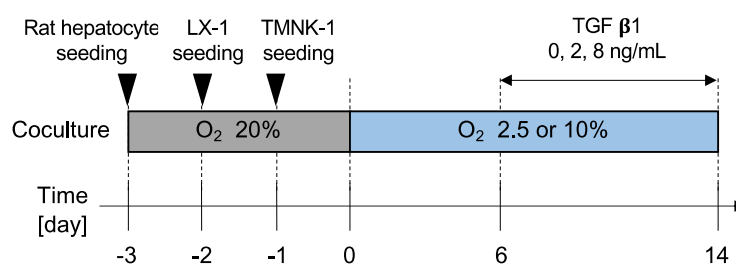


**Figure 1.** Experimental schedule of coculture and stimulation by TGF-β1.

### 2.5. Fibrogenesis induction under low oxygen tension and exposure to the pro-fibrogenic cytokine

From day 0 onward, oxygenation tensions were varied from 20% to 10% physiological oxygenation level and 2.5% low oxygenation condition [25]. Fibrogenesis was further induced on day 6 with the pro-fibrogenic cytokine, TGF-β1, at 2 and 8 ng/ml until day 14, which marked the end of the experiment.

### 2.6. Measurement of albumin production

The culture supernatant was collected, and the amount of albumin secreted in the culture medium was determined using the sandwich-type enzyme-linked immunosorbent assay (ELISA) [26]. Goat anti-rat albumin antibody (Bethyl, USA) was used as the primary antibody, and a horseradish peroxidase-conjugated sheep anti-rat albumin (Bethyl, USA) was used as the secondary antibody. The absorbance was measured by the microplate reader iMark (Bio-Rad, USA) at 490 nm with an optical correction of 630 nm.

### 2.7. Cytochrome P450 (CYP) 3A4 activity assay

Rat CYP3A4 activity was determined on day 6 and day 14 of the culture using the P450-Glo CYP3A4 assay kit (Promega, USA). Williams' Medium E was aspirated from cultured wells, and fresh Williams' Medium E containing Luciferin-3A4 (1:1000) was added to the wells and incubated for 1 h in a 37°C incubator at their respective oxygen tension. 25 μl of culture medium containing metabolite from each well was transferred to opaque 96-well white luminometer plates, and 25 μl of Luciferin Detection Reagent was added to initiate a luminescent reaction. Plates were incubated at room temperature for 20 min away from light, and the luminescence was subsequently read using the Wallac 1420 ARVO SX microplate luminometer (PerkinElmer, USA).

### 2.8. Real-time quantitative polymerase chain reaction

Total RNAs were isolated from tissue culture samples using the TRIzol reagent (Life Technologies, USA) and purified using the Direct-zol RNA MiniPrep kit (Zymo Research, USA) according to the manufacturer's instructions. The concentration and quality of each RNA sample

were assessed with the BioSpec-nano spectrophotometer (Shimadzu, Japan). Complementary DNAs (cDNAs) were reverse-transcribed from 100 ng total RNA samples using the ReverTra Ace qPCR RT Master Mix with gDNA Remover (Toyobo, Japan). Real-time quantitative polymerase chain reaction (qRT-PCR) assays were then performed with the THUNDERBIRD SYBR qPCR Mix (Toyobo, Japan) and assessed using the real-time StepOnePlus qPCR system (Applied Biosystems, USA). Primer sequences used for the real-time qPCR are shown in Table 1, with human and rat  $\beta$ -actin serving as the internal controls.

**Table 1.** List of qRT-PCR primers.

Species	Gene	Forward Primer Sequences	Reverse Primer Sequences
Human	$\beta$ -actin	CCTCATGAAGATCCTCACCGA	TTGCCAATGGTGATGACCTGG
	$\alpha$ -SMA	AGGCACCCCTGAACCCCAA	CAGCACCGCCTGGATAGCC
	Col1A1	CCAAATCTGTCTCCCCAGAA	TCAAAAACGAAGGGGAGATG
	Col3A1	TGGTCTGCAAGGAATGCCTGGA	TCTTTCCCTGGGACACCATCAG
	Col4A1	CCTGGCTTGAAAAACAGCTC	CCCTGCTGAGGTCTGTGAAC
	PDGF	ATGATCTCCAACGCCTGC	TCAGCAATGGTCAGGGAAC
	TIMP1	CAAGATGTATAAAGGGTTCCAAGC	TCCATCTGCAGTTTTCCAG
	MMP2	AAGTATGGCTTCTGCCCTGA	ATTTGTTGCCAGGAAAGTG
	CTGF	AATGCTGCGAGGAGTGGGT	CGGCTCTAATCATAGTTGGGTCT
	$\beta$ -actin	AGAGAAGCTGTGCTATGTTGC	GTA CTCTGCTTGCTGATCC
Rat	CYP1A1	GATGCTGAGGACCAGGAAGACCGC	CAGGAGGCTGGACGAGAATGC
	CYP1A2	CTTGGAGAAGCGTGGCCAGG	CTACAAAGACAACGGTGGTCT

### 2.9. Vertical cross-section, H&E staining, AZAN staining, and immunostaining

Cell-loaded PDMS discs were collected and fixed with 4% paraformaldehyde solution (FUJIFILM Wako Pure Chemical, Japan) in PBS overnight, and the cell sheets were rinsed thoroughly with PBS. Fixed samples were performed paraffin-embedded, sliced in 5 mm thickness, and stained with hematoxylin and eosin (H & E) or azocarmine and aniline blue (AZAN) by GENOSTAFF CO., LTD. (Tokyo Japan). Images were captured using a transmitted light microscope BX50 (Olympus, Japan).

For the immunostaining, tissue samples were fixed with 4% paraformaldehyde (PFA) (Wako, Japan) at room temperature for 30 min and thoroughly washed with PBS to remove the PFA. The 1% Triton X-100 (Wako, Japan) was added and incubated for 30 min for permeabilization. After washing with PBS, tissue samples were further incubated with a gelatin blocking buffer for 1 h, followed by incubation with mouse anti-human alpha-smooth muscle actin ( $\alpha$ -SMA) monoclonal antibody (1:1000; Agilent Dako, USA) and goat anti-type I collagen antibody (1:1000; SouthernBiotech, USA) overnight at 4°C. Samples were washed with PBS and subsequently incubated with donkey anti-mouse IgG H&L (Alexa Fluor® 488) antibody (1:100; Invitrogen, USA), and donkey anti-goat IgG H&L (Alexa Fluor® 647) antibody (1:100; Invitrogen, USA) for 1 h at room temperature while protected from light. After washing with PBS, samples were counterstained with 4',6-diamidino-2-phenylindole (DAPI) (1:1000) (Dojindo, Japan) for 15 min and washed again with PBS. Fluorescent images were taken using a confocal laser scanning microscope FLUOVIEW FV3000 (Olympus, Japan).

### 2.10. Statistical analysis

Data are represented as the mean  $\pm$  standard deviation (SD). Statistical analysis was performed by GraphPad Prism 8.3.0 (GraphPad, California, U.S.) to determine the statistical significance of the

albumin production, CYP3A4 activity, and qPCR results with  $p^* < 0.05$  and  $p^{**} < 0.01$  as statistically significant and  $p^{***} < 0.001$  and  $p^{****} < 0.0001$  as highly significant, respectively.

### 3. Results

#### 3.1. Hierarchical coculture structure was intact for two weeks and acquired better functionalities than hepatocyte monoculture

The hierarchical cocultured liver tissue consisting of LX-2 and TMNK-1 was cultured up to day 14 without detachment. In contrast, hepatocyte monocultures started to clump and detach from the PDMS surface from day 4 onward suggesting that the coculture system had promoted cell-cell interaction and enhanced stability of cocultured liver tissues. Although no morphological changes were observed between the cocultures in 2.5% and 10% oxygenation conditions, a thicker tissue was formed under a 10% oxygen tension, as shown in the HE and AZAN histological staining (Figure 2A).

The hepatocyte monoculture and the cocultured liver tissue were tested to confirm the differences in hepatocytes' hepatic function in these cultures. Albumin secretion in cocultures at both 10% and 2.5% oxygenation conditions was higher than monocultures for the entire culture period of 14 days (Figure 2B). As for the cocultures at 2.5% oxygenation condition, albumin secretion reached the maximum on day 8, and then it rapidly decreased. At 10% oxygenation condition, albumin secretion reached the maximum on day 12 and maintained that high production level until day 14. By the end of day 14, the cocultures in 10% oxygenation level had an albumin protein secretion level of about 1.8-fold higher than that of hepatocyte monocultures, and cocultures in 2.5% oxygenation level had an albumin protein secretion level of about 2.1-fold higher than that of hepatocyte monocultures.

The hepatic cytochrome P450 (CYP) 3A4 activities of cell line cocultures were also higher than hepatocyte monocultures on day 6 (Figure 2C). We then proceeded to use the cocultured liver tissue for inflammation studies.

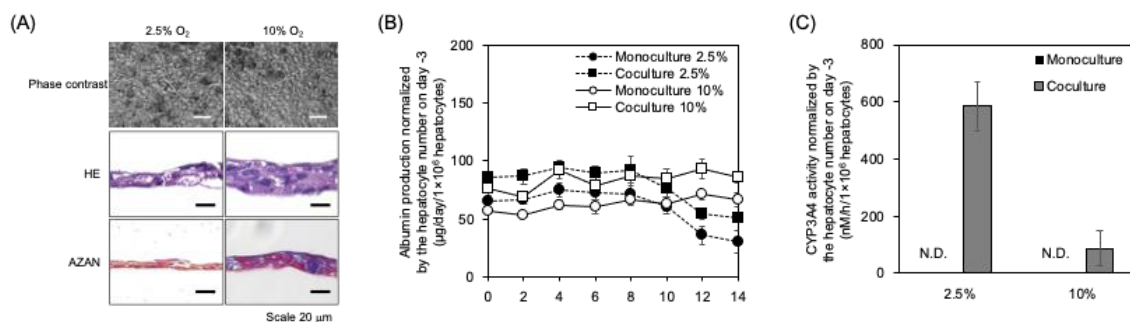


**Figure 2.** Morphological and functional comparison of hierarchical cocultured liver tissue under 2.5% and 10% oxygen tension. (A) Morphology of coculture on day 14. (B) Albumin production during the culture. (C) CYP3A4 activity of monocultures and cocultures in 2.5% and 10% oxygen tension on day 6.

#### 3.2. Liver functions were well expressed in different oxygen tensions, and CYP3A4 activity was influenced by TGF-β1 stimulation

In comparing cocultures under different oxygen tensions, cocultures in 2.5% oxygen tension had a lower albumin protein secretion level than that of the cocultures in 10% oxygenation level on day 14 (Figure 3A). Moreover, the cocultures in 2.5% oxygenation condition exhibited higher CYP3A4 activity than 10% oxygenation condition on day 6 and day 14 (Figure 2C and 3B).

After eight days of stimulation by TGF- $\beta$ 1, no distinct differences were observed in albumin secretion on day 14 for both the 10% and 2.5% oxygen tension groups (Figure 3A). CYP3A4 activity levels were also similar between day 6 and day 14 in the group without TGF- $\beta$ 1 stimulation and at 2 ng/mL stimulation (Figure 3B), while it decreased in 8 ng/mL of TGF- $\beta$ 1 stimulation groups at both 2.5% and 10% oxygen tensions. CYP1A1 and CYP1A2 (Figure 3C and 3D) were unchanged by TGF- $\beta$ 1 stimulation, suggesting no strong correlation in the respective CYP expressions to the stimulus with TGF- $\beta$ 1.

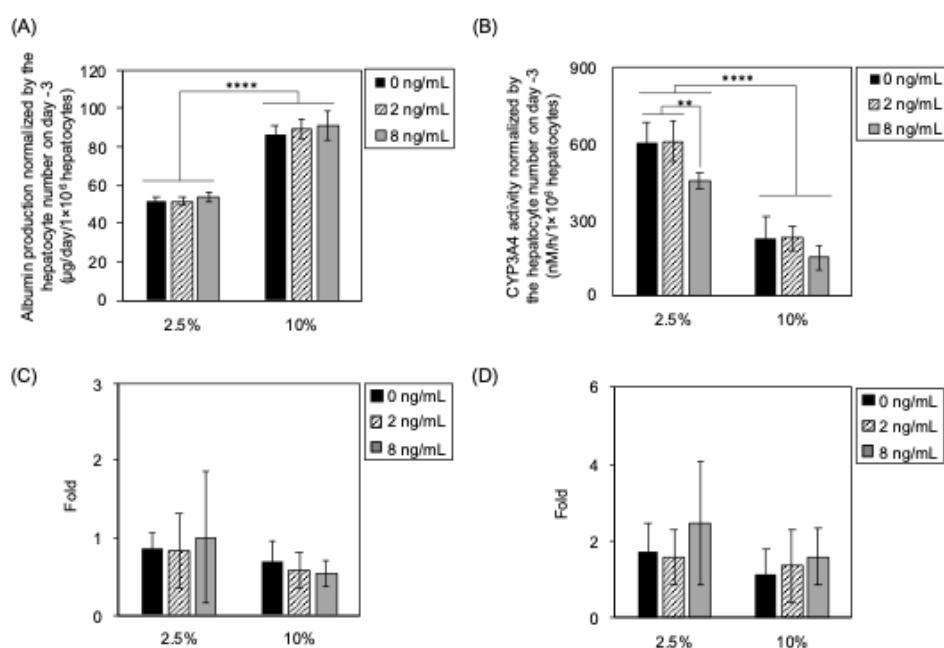


**Figure 3.** Evaluation of hepatic function in 2.5% and 10% oxygen tension with TGF- $\beta$ 1 stimulation (0, 2, 8 ng/mL) on day 14. (A) and (B) Albumin production and CYP3A4 activity of cocultures in 2.5% and 10% oxygen tension, respectively. Data represent the mean  $\pm$  standard deviation (SD, n = 6) from two independent experiments. Each value was normalized to hepatocyte number on day -3. Statistical significance was determined by the one-way ANOVA method with Tukey's multiple comparison test with statistical significance of \*p < 0.05, \*\*p < 0.01, \*\*\*p < 0.001, and \*\*\*\*p < 0.0001. (C) and (D) Relative gene expression of CYP1A1 and CYP1A2 of cocultures in 2.5% and 10% oxygen tension with TGF- $\beta$ 1 stimulation (0, 2, 8 ng/mL) on day 14. Each dataset represents the mean  $\pm$  standard deviation (SD, n = 6) from two independent experiments. Statistical significance was determined by the one-way ANOVA method with Tukey's multiple comparison test with statistical significance of \*p < 0.05, \*\*p < 0.01, \*\*\*p < 0.001, and \*\*\*\*p < 0.0001.

### 3.3 Cocultured tissues were induced fibrogenesis by pro-fibrotic cytokine stimulation

We stimulated cocultured liver tissues with the pro-fibrotic cytokine, TGF- $\beta$ 1, for eight days from day 6 (Figure 1) and analyzed the mRNA expression of key fibrotic-related genes to characterize the response of HSCs in the cocultured liver tissues. The impact of low oxygen tension stimulation on inducing inflammation and possible fibrogenesis was also examined by the relative gene expression of HSC activation-related and fibrosis-related biomarkers on both day 6 and day 14.

Gene expression of several biomarkers showed slight upregulation in 2.5% compared to 10% oxygenation condition on day 6 (Figure 4). However, these increases in gene expression were not observed on day 14, except for the alpha-smooth muscle actin ( $\alpha$ -SMA) and connective tissue growth factor (CTGF) biomarkers (Figure 5).

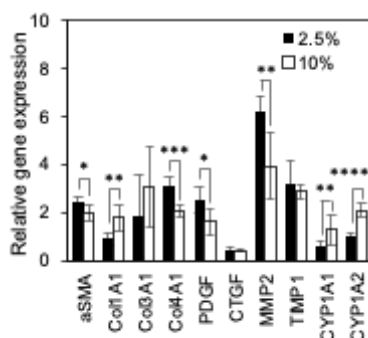


**Figure 4.** Relative gene expression of cocultures in 2.5% and 10% oxygen tension on day 6 normalized to day 0 coculture. Each dataset represents the mean  $\pm$  standard deviation (SD, n = 6) from two independent experiments. Statistical significance was determined by the Student's t-test with statistical significance of \*p < 0.05, \*\*p < 0.01, \*\*\*p < 0.001, and \*\*\*\*p < 0.0001.



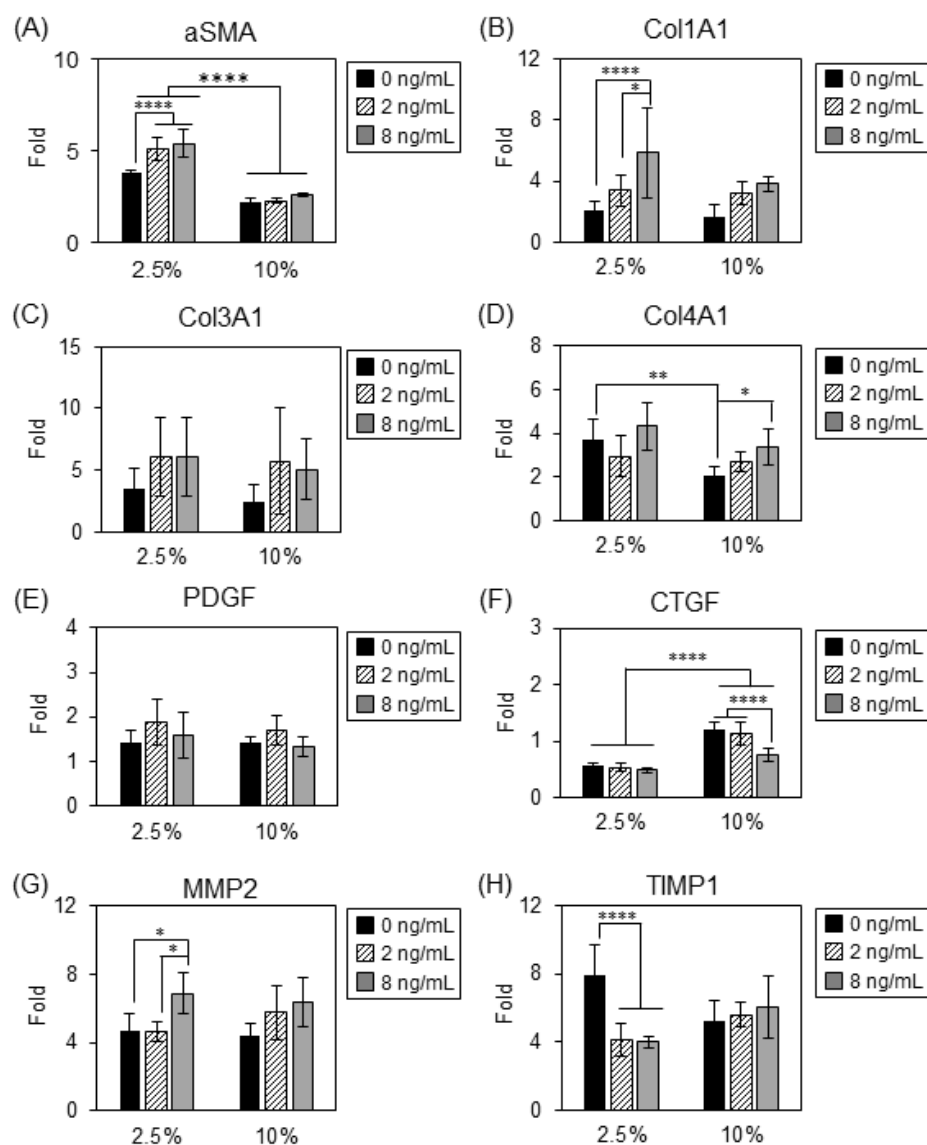


**Figure 5.** Relative gene expression of cocultures in 2.5% and 10% oxygen tension with TGF-β1 stimulation (0, 2, 8 ng/mL) on day 14. Each dataset represents the mean ± standard deviation (SD, n = 6) from two independent experiments. Statistical significance was determined by the one-way ANOVA method with Tukey's multiple comparison test with statistical significance of \* $p < 0.05$ , \*\* $p < 0.01$ , \*\*\* $p < 0.001$ , and \*\*\*\* $p < 0.0001$ .

The activation of HSCs is accompanied by the upregulation in the expression of fibrosis-related genes such as  $\alpha$ -SMA [27,28]. For  $\alpha$ -SMA gene expression, there was a significant increase in the coculture from day 0 at 20% oxygenation tension to day 6 at both 10% and 2.5% oxygenation tensions. On day 6, there was also a slight upregulation in the  $\alpha$ -SMA gene expression when the coculture was exposed to 2.5% low oxygenation tension as compared to 10% (Figure 4). Upon continuous low oxygen tension stimulation, on day 14, there was a further increase in the  $\alpha$ -SMA gene expression for the cocultures in the 2.5% oxygen tension group compared to those in the 10% group (Figure 5A). Further stimulation by TGF-β1 resulted in enhanced  $\alpha$ -SMA gene expression, especially in the 2.5% oxygen tension group. However,  $\alpha$ -SMA immunostaining results revealed no significant differences between cocultures cultured under 2.5% and 10% oxygen tension (Figure 6). These results indicated that continuous treatment at a low oxygen concentration of 2.5% with a higher concentration of TGF-β1 stimulation possibly resulted in a slight overall increase in the activation of HSCs.

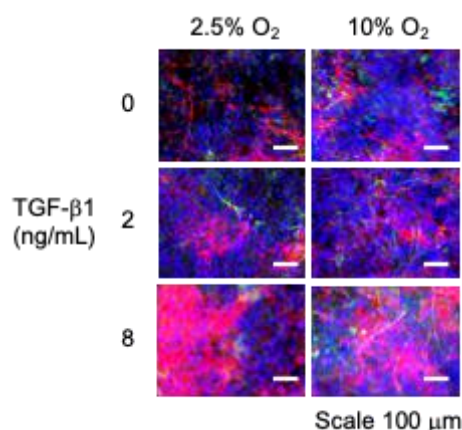


**Figure 6.** Immunostaining of cocultures in 2.5% and 10% oxygen tension with TGF- $\beta$ 1 stimulation (0, 2, 8 ng/mL) on day 14. Green, red, and blue are  $\alpha$ -SMA, collagen type I, and DAPI, respectively.

Fibrosis is characterized by the extensive deposition of ECM proteins, mainly collagen type I, III, and IV produced by HSCs [1,22,27,29,30]. The gene expression level of collagen type I was upregulated on day 6 for cultures subjected to 10% oxygenation tension as compared to day 0 cocultures; however, an increase in the collagen type I gene expression was not observed for the cocultures subjected to 2.5% oxygen tension (Figure 4). On day 14, the collagen type I gene expression remained relatively constant for the 10% oxygenation tension group. However, there was an increase in collagen type I gene expression for the 2.5% oxygenation tension group compared to day 6, even though there was no significant difference in the collagen type I gene expression on day 14 concerning the change in oxygen tension (Figure 5B). Collagen type I gene, Col1A1 expression, had a concentration-dependent change with TGF- $\beta$ 1 on day 14 (Figure 5B). Furthermore, immunostaining results also showed a higher expression of collagen type I at 8 ng/ml (Figure 6). Similar trends could also be observed in the collagen type III (Col3A1) and IV (Col4A1) gene expression results (Figure 5C and 5D). Increases in the gene expressions from day 0 control cocultures at 20% oxygenation tension to day 6 cocultures at 10% and 2.5% oxygenation tensions were observed. Upon continuous hypoxic stimulation, on day 14, there was a significant increase in the gene expression for collagen type IV in the cocultures under the 2.5% oxygen tension group compared to the 10% group (Figure 5D). Col3A1 and Col4A1 gene expression also tended to increase by TGF- $\beta$ 1 stimulation, while there were no statistical differences (Figure 5C and 5D). These results illustrated that higher TGF- $\beta$ 1 stimulation concentrations resulted in collagen fiber synthesis and collagen accumulation in the cocultured liver tissues.

Platelet-derived growth factor gene, PDGF expression is upregulated during the proliferation of activated HSCs and is a marker for HSC proliferation [28,31]. The effect of varying oxygen tension on PDGF gene expression was observed on day 6 as there was generally an increase in PDGF expression for both the 2.5% and 10% oxygenation tension groups compared to 20% oxygen tension on day 0 (Figure 4). However, this continual variation of oxygen tension and TGF- $\beta$ 1 stimulation did not cause further change in the PDGF gene expression on day 14 (Figure 5E).

CTGF gene expression levels were relatively stable at both 2.5% and 10% oxygenation tensions (Figure 4). There was no further significant change in CTGF gene expression under hypoxia treatment of 2.5% oxygen tension on day 14; however, culturing at 10% physiological oxygenation level increased the gene expression by about 3.0-fold compared to that on day 6 (Figure 5F).

For MMP2 gene expression, a significant increase in both the 2.5% oxygenation tension group and the 10% oxygenation tension group on day 6 relative to the 20% oxygenation tension control group on day 0 was observed (Figure 4). After prolonged treatment at 2.5% low oxygen tension, no significant influence on MMP2 gene expression could be observed on day 14. However, the gene

expression increased significantly when the cocultured liver tissues were induced with 8 ng/ml of TGF- $\beta$ 1 at 2.5% and 10% oxygen tension (Figure 5G). As for TIMP1 gene expression, with varying oxygen tension alone, there was an upregulation on day 6 in both the 10% and 2.5% oxygen tension cocultures than the control cocultures at 20% oxygenation on day 0 (Figure 4). Upon prolonged hypoxia treatment at 2.5% low oxygen tension, TIMP1 gene expression was further enhanced compared to 10% oxygen tension on day 14 (Figure 5H), suggesting that prolonged low oxygen tension treatment resulted in a promotion of collagen synthesis in the coculture tissues.

#### 4. Discussion

We demonstrated the liver coculture system of hepatocytes and non-parenchymal liver cells, including HSCs and LSECs, for potential liver fibrogenesis studies. We intended to mimic the *in vivo* microenvironment and developed the hierarchical cocultured liver tissues inspired by the microstructure surrounding the hepatocytes by seeding hepatocytes, HSCs, and LSECs, one on top of the other on oxygen-permeable PDMS membranes. Lower oxygen tension and TGF- $\beta$ 1 stimulation activate HSCs (LX-2) in our coculture system resulting in the rise of collagen type I and alpha-smooth muscle actin markers. As a result, this *in vitro* hierarchical cocultured liver tissue could possibly be utilized as a disease model for liver fibrogenesis studies.

Over the years, scientific development has focused on establishing relevant anti-fibrotic strategies that target the HSCs [32]. However, such 2D monoculture models have been proven to be inefficient in developing appropriate treatments for control of liver damage as the mechanisms by which HSCs are mediated through culture might differ considerably despite the application of different HSC culture models of varying complexity [33–35]. Thus, much needed to be incorporated to justify the treatment of chronic liver conditions. Research showed a significant interaction between HSCs, biomechanics, cell-matrix, hepatocytes, and other non-parenchymal cells that enhance and promote specific liver cell functions [32]. As such, the development of 3D *in vitro* models that could recreate the liver microenvironment is required and could be linked to the objectives of developing novel anti-fibrogenic compounds.

Utilizing such a PDMS-based culture system enables the supply of sufficient oxygen content to the tissue, which leads to maintaining viability and promoting the healthy growth of liver tissues to develop high-density 3D cell culture [17,36–38]. As cultured primary rat hepatocytes exhibit high oxygen consumption [39], the PDMS culture plate allows the establishment of a hierarchical coculture model that mimics the *in vivo* liver physiology as primary hepatocytes could be easily cocultured with other non-parenchymal cells in a 3D manner or structure using this platform [17,36]. On the contrary, conventional tissue culture polystyrene plates could not support this kind of coculture due to insufficient oxygen being supplied to the tissues to maintain viability and growth [40]. Other coculture systems or studies have also encountered the limited formation of cell-cell contacts [41–43], and oxygen shortage could limit the thick tissue formation and the hepatic functions of the cocultures [44]. Based on our culture system, while hepatocyte and LX-2 monocultures started to aggregate and detach from the culture plates' PDMS surfaces after day 4, we managed to characterize the cocultured liver tissue functions such as albumin production, metabolic enzyme activity, and gene expression. Cocultures maintained cellular attachment and their hepatic functions better than monocultures, as there was an enhancement in albumin protein synthesis and activity of rat drug metabolism enzyme, CYP3A4 (Figure 2B and 2C). It has been reported that the cell-cell interaction enhanced hepatic function by promoting the cell-derived growth factor or ECM production [45]. Thus, the studied cocultured tissues might promote tissue formation with enhanced cell-matrix production. Since PDMS-based culture enables direct oxygenation to the cultured cells in different oxygen tensions without oxygen shortage for cellular respiration [37,38], we then varied the culture atmosphere from 20% to 10% and 2.5% oxygen tension (Figure 1). The liver has an oxygen tension-dependent behavior, and its function is influenced by the oxygen gradient [46,47]. The lower oxygen tension area is near the central vein, and the higher oxygen tension area is near the portal vein [46,47]. The oxygen supply

---

at physiological conditions enhances multiple hepatocyte inductive factors that might promote albumin production in liver tissues [48]. Moreover, CYP P450 activity is influenced by oxygen gradient and low oxygen regions. Therefore, albumin production and CYP3A4 expression are higher in the area of portal vein and central vein, respectively. In our results, we demonstrated that albumin production decreased under 2.5% low oxygen tension, while CYP3A4 activity increased in the cocultures (Figure 3A and 3B). Albumin production and CYP3A4 activity showed oxygen tension-dependent behavior due to the continuous oxygenation even in low oxygen tension condition [46,47].

The cocultured liver tissue was then applied to the examination of further fibrogenesis studies by TGF- $\beta$  stimulation. During chronic liver injury, the increased accumulation of ECM, which is generally rich in both type I and III collagen, results in liver fibrosis and scar deposition [28,30,49,50]. During fibrogenesis, HSCs, which are localized in the perisinusoidal space between the sinusoidal endothelial cells and the hepatocytes, transdifferentiate to myofibroblasts with their activation [2,49]. A wide range of collective and individual signals, as well as intracellular occurrences, could lead to HSC activation. Some of the significant proliferative and fibrogenic pathways regulating the activation of HSCs include cytokines such as the connective tissue growth factor (CTGF), platelet-derived growth factor (PDGF), transforming growth factor- $\beta$  (TGF- $\beta$ ) [12], and the vascular endothelial growth factor (VEGF) [49]. TGF- $\beta$  is recognized as the most potent fibrogenic cytokine, which, in a quiescent form, is produced by several cell populations found in the liver [51]. The phosphorylation of the type I receptor, along with TGF- $\beta$  binding, is known to induce phosphorylation of downstream SMAD proteins, primarily of SMAD3 [49]. When SMAD3 is activated during HSC activation, it elevates the transcription of type III and type I collagen [12,52,53]. Hypoxia is another commonly regarded environmental stress factor that is closely linked to several pathological and physiological conditions like fibrogenesis, according to Shi et al. [11]. Liver injuries occur in the hypoxic regions, and HSC activation is considered the critical aspect of liver fibrogenesis [11].

We observed an upregulation of the fibrosis-related biomarkers and HSC activation markers such as  $\alpha$ -SMA [28] when we subjected the model to a low oxygen tension condition and the pro-fibrogenic cytokine, TGF- $\beta$ 1 (Figure 4 and 5A). Interestingly, our results showed that continuous treatment alone at a low oxygen tension of 2.5% could result in an overall increase in the activation of HSCs, as observed with the rise in  $\alpha$ -SMA gene expression in the cocultures (Figure 4). Furthermore, when stimulated with TGF- $\beta$ 1, there was a further increase not only in the  $\alpha$ -SMA gene expression but also in other fibrosis biomarkers such as collagen type I, III, and IV [1,22,29] that are commonly found in diseased livers, indicating that TGF- $\beta$ 1 had a substantial pro-fibrogenic effect on the coculture system. TIMP1 is responsible for the inhibition of MMPs (which degrades ECM) [1,54–57], thus leading to a net accumulation of ECM in fibrotic livers. TIMP1 gene expression was increased after continuous culture under both high and low oxygen tensions. Collectively, these results demonstrated that low oxygen tension, coupled with TGF- $\beta$  stimulation, had resulted in a greater extent of HSC activation in vitro and that further stimulation by TGF- $\beta$  should promote their fibrogenesis with excessive collagen production and accumulation. We also noted that the enhancement of PDGF gene expression, a marker for activated HSC proliferation [2,28,49,58], with an upregulation of the gene observed throughout the whole coculture period, suggesting that there was a proliferation of activated HSCs in the coculture in vitro. Albumin protein secretion, expression of genes encoding for CYP enzymes, and its activity were studied to evaluate the possible effect of TGF- $\beta$ 1 stimulation on the cocultured liver tissue's functional characteristics. As shown in the results, there was no conclusive evidence that varying TGF- $\beta$ 1 stimulation concentrations would affect the rat albumin secretion and expression of rat drug-metabolism enzymes, such as CYP1A1/1A2/3A4, as there was no significant decrease in their expressions after stimulating with the pro-fibrotic TGF- $\beta$ 1 cytokine. This indicates rat hepatocytes' functionality in the cocultures; hence, the tissues' hepatic function was not affected because of the relatively constant gene expression and maintenance of crucial rat functionality indexes.

---

Although 3D multicellular spheroids overcome many monoculture or in vitro 2D culture systems' limitations by increasing viability, enhancing parenchymal-non parenchymal cell-to-cell interactions, and normal tissue phenotype [59], limitations exist for spheroid cultures. Mainly, when larger cell sizes are used, inner cells degenerate easily [60] as the diffusion gradient of nutrients, oxygen, and compounds across the spheroids would limit exposure to the inner cells, which could lead to the formation of necrotic core in the spheroids [61]. Metabolic waste accumulation occurs as well due to inefficient mass transport [62]. On the contrary, this kind of hierarchical coculture system has its advantages due to its accessibility to nutrients and test compounds, and the flexibility to include different cell types could be extended to coculturing of cells in microphysiological systems for developing assays for high-throughput screening. Overall, through stable culturing of the major heterogeneous cells that make up the liver, the system becomes more stable than the hepatocyte monoculture. In particular, by administering inflammatory cytokines and intentionally blocking oxygen supply to cells, we have observed the activation of hepatic stellate cells and the enhanced synthesis and accumulation of collagen fibers in the culture system, as seen in the early stages of liver fibrogenesis. Though further study about the influence of cellular-derived factors should be examined, this culture system holds great promise. It could be used not only to observe the effects and side effects of drugs but also to reproduce the liver fibrogenesis phenomenon, which is attracting attention as a chronic liver disease mechanism under culture conditions. Besides, the use of human primary hepatocytes or human-derived parenchymal hepatocytes and non-parenchymal hepatic cells from other cell sources like induced-pluripotent stem cells could be employed to establish an even more physiologically relevant in vitro human liver fibrosis model in the future.

## 5. Conclusions

We developed multilayer cocultured liver tissues with hepatocyte, sinusoidal endothelial cells, and hepatic stellate cells to demonstrate the induction of liver inflammation for liver fibrosis models in vitro. Our cocultured liver tissues maintained their hepatic functions and showed their utility and capability as a physiologically relevant disease model to respond to the pro-fibrotic factor, TGF- $\beta$ 1, stimulation. Although the collagen synthesis and degradation-related gene expression were not consistent, hypoxia-induced hepatic disorder and TGF- $\beta$ 1-dependent fibrogenesis behavior in gene expressions were observed. This culture system demonstrated the potential application to examine the molecular mechanisms and pathogenesis of liver fibrosis, cellular interaction, and unknown microenvironmental factors, which would lead to the development of novel anti-fibrogenic strategies and potent drugs to stimulate liver recovery. Further studies using a combination of human cells, including immune cells, are expected.

**Author Contributions:** Conceptualization, Y.S., M.S., and Q.Y.L.; methodology, Y.S., M.S., and Q.Y.L.; validation, Q.Y.L. and F.G.T.; formal analysis, Q.Y.L., F.G.T., and M.S.; data curation, Q.Y.L., F.G.T., and M.S.; writing—original draft preparation, Q.Y.L., F.G.T., and M.S.; writing—review and editing, Q.Y.L., F.G.T., M.S., and Y.S.; supervision, Y.S. and M.S.; project administration, Y.S. and M.S.; funding acquisition, Y.S. and M.S. All authors have read and agreed to the published version of the manuscript.

**Funding:** This research was funded by the Japanese Agency for Medical Research and Development (Grant No. 18bm0704007h0003 and 17be0304201h0001) and Japan Bio Products Co., Ltd.

**Acknowledgments:** We would like to especially thank Dr. Hiroyuki Miyazaki, from Japan Bio Products Co., Ltd., for his technical advice.

**Conflicts of Interest:** The authors declare no conflict of interest. The funders had no role in the design of the study; in the collection, analyses, or interpretation of data; in the writing of the manuscript, or in the decision to publish the results.

## References

1. Robert, S.; Gicquel, T.; Bodin, A.; Lagente, V.; Boichot, E. Characterization of the MMP/TIMP imbalance and collagen production induced by IL-1  $\beta$  or TNF- $\alpha$  release from human hepatic stellate cells. *PLoS ONE* **2016**, *11*, 1–14, doi:10.1371/journal.pone.0153118.
  2. Puche, J.E.; Saiman, Y.; Friedman, S.L. Hepatic stellate cells and liver fibrosis. *Compr. Physiol.* **2013**.
  3. Friedman, S.L.; Sheppard, D.; Duffield, J.S.; Violette, S. Therapy for fibrotic diseases: nearing the starting line. *Sci. Transl. Med.* **2013**, *5*, 167sr1–167sr1.
  4. Schuppan, D.; Kim, Y.O. Evolving therapies for liver fibrosis. *J. Clin. Invest.* **2013**, *123*, 1887–1901.
  5. Greek, R.; Menache, A. Systematic reviews of animal models: methodology versus epistemology. *Int. J. Med. Sci.* **2013**, *10*, 206.
  6. Schuster, D.; Laggner, C.; Langer, T. Why drugs fail—a study on side effects in new chemical entities. *Curr. Pharm. Des.* **2005**, *11*, 3545–3559.
  7. Müller, F.A.; Sturla, S.J. Human in vitro models of nonalcoholic fatty liver disease. *Curr. Opin. Toxicol.* **2019**, *16*, 9–16.
  8. Bhandari, R.N.B.; Riccalton, L.A.; Lewis, A.L.; Fry, J.R.; Hammond, A.H.; Tendler, S.J.B.; Shakesheff, K.M. Liver Tissue Engineering: A Role for Co-culture Systems in Modifying Hepatocyte Function and Viability. *Tissue Eng.* **2001**, *7*, 345–357, doi:10.1089/10763270152044206.
  9. Block, G.D.; Locker, J.; Bowen, W.C.; Petersen, B.E.; Katyal, S.; Strom, S.C.; Riley, T.; Howard, T.A.; Michalopoulos, G.K. Population expansion, clonal growth, and specific differentiation patterns in primary cultures of hepatocytes induced by HGF/SF, EGF and TGF  $\alpha$  in a chemically defined (HGM) medium. *J. Cell Biol.* **1996**, *132*, 1133–1149, doi:10.1083/jcb.132.6.1133.
  10. Shulman, M.; Nahmias, Y. Long-term culture and coculture of primary rat and human hepatocytes. In *Epithelial Cell Culture Protocols*; Springer, 2012; pp. 287–302.
  11. Shi, Y.F.; Fong, C.C.; Zhang, Q.; Cheung, P.Y.; Tzang, C.H.; Wu, R.S.S.; Yang, M. Hypoxia induces the activation of human hepatic stellate cells LX-2 through TGF- $\beta$  signaling pathway. *FEBS Lett.* **2007**, *581*, 203–210, doi:10.1016/j.febslet.2006.12.010.
  12. Xu, F.; Liu, C.; Zhou, D.; Zhang, L. TGF- $\beta$ /SMAD Pathway and Its Regulation in Hepatic Fibrosis. *J. Histochem. Cytochem.* **2016**, *64*, 157–167.
  13. Bhadriraju, K.; Chen, C.S. Engineering cellular microenvironments to improve cell-based drug testing. *Drug Discov. Today* **2002**, *7*, 612–620.
  14. Breslin, S.; O'Driscoll, L. Three-dimensional cell culture: the missing link in drug discovery. *Drug Discov. Today* **2013**, *18*, 240–249.
  15. Breslin, S.; O'Driscoll, L. The relevance of using 3D cell cultures, in addition to 2D monolayer cultures, when evaluating breast cancer drug sensitivity and resistance. *Oncotarget* **2016**, *7*, 45745.
  16. Bell, C.C.; Hendriks, D.F.G.; Moro, S.M.L.; Ellis, E.; Walsh, J.; Renblom, A.; Fredriksson Puigvert, L.; Dankers, A.C.A.; Jacobs, F.; Snoeys, J.; et al. Characterization of primary human
-

- hepatocyte spheroids as a model system for drug-induced liver injury, liver function and disease. *Sci. Rep.* **2016**, *6*, 25187, doi:10.1038/srep25187.
17. Xiao, W.; Perry, G.; Komori, K.; Sakai, Y. New physiologically-relevant liver tissue model based on hierarchically cocultured primary rat hepatocytes with liver endothelial cells. *Integr Biol* **2015**, *7*, 1412–1422, doi:10.1039/C5IB00170F.
  18. Bhatia, S.N.; Balis, U.J.; Yarmush, M.L.; Toner, M. Probing heterotypic cell interactions: hepatocyte function in microfabricated co-cultures. *J. Biomater. Sci. Polym. Ed.* **1998**, *9*, 1137–1160.
  19. Bhatia, S.N.; Balis, U.J.; Yarmush, M.L.; Toner, M. Effect of cell--cell interactions in preservation of cellular phenotype: cocultivation of hepatocytes and nonparenchymal cells. *FASEB J.* **1999**, *13*, 1883–1900.
  20. Nuciforo, S.; Heim, M.H. Organoids to model liver disease. *JHEP Rep.* **2020**, 100198.
  21. Du, Y.; Li, N.; Yang, H.; Luo, C.; Gong, Y.; Tong, C.; Gao, Y.; Lü, S.; Long, M. Mimicking liver sinusoidal structures and functions using a 3D-configured microfluidic chip. *Lab. Chip* **2017**, *17*, 782–794.
  22. Gressner, A.M.; Weiskirchen, R. Modern pathogenetic concepts of liver fibrosis suggest stellate cells and TGF- $\beta$  as major players and therapeutic targets. *J. Cell. Mol. Med.* **2006**, *10*, 76–99.
  23. Seglen, P.O. Preparation of isolated rat liver cells. In *Methods in cell biology*; Elsevier, 1976; Vol. 13, pp. 29–83.
  24. Xu, L.; Hui, A.Y.; Albanis, E.; Arthur, M.J.; O'byrne, S.M.; Blaner, W.S.; Mukherjee, P.; Friedman, S.L.; Eng, F.J. Human hepatic stellate cell lines, LX-1 and LX-2: new tools for analysis of hepatic fibrosis. *Gut* **2005**, *54*, 142–151.
  25. Yan, H.-M.; Ramachandran, A.; Bajt, M.L.; Lemasters, J.J.; Jaeschke, H. The oxygen tension modulates acetaminophen-induced mitochondrial oxidant stress and cell injury in cultured hepatocytes. *Toxicol. Sci.* **2010**, *117*, 515–523.
  26. Hanada, S.; Kayano, H.; Jiang, J.; Kojima, N.; Miyajima, A.; Sakoda, A.; Sakai, Y. Enhanced in vitro maturation of subcultivated fetal human hepatocytes in three dimensional culture using poly-L-lactic acid scaffolds in the presence of oncostatin M. *Int. J. Artif. Organs* **2003**, *26*, 943–951.
  27. Kisseleva, T.; Brenner, D.A. Hepatic stellate cells and the reversal of fibrosis. *J. Gastroenterol. Hepatol. Aust.* **2006**, *21*, doi:10.1111/j.1440-1746.2006.04584.x.
  28. Moreira, R.K. Hepatic Stellate Cells and Liver Fibrosis. *Arch Pathol Lab Med—Vol* **2007**, *131*, 1728–1734, doi:10.1002/cphy.c120035.
  29. Urushiyama, H.; Terasaki, Y.; Nagasaka, S.; Terasaki, M.; Kunugi, S.; Nagase, T.; Fukuda, Y.; Shimizu, A. Role of  $\alpha 1$  and  $\alpha 2$  chains of type IV collagen in early fibrotic lesions of idiopathic interstitial pneumonias and migration of lung fibroblasts. *Lab. Invest.* **2015**, *95*, 872.
  30. Bataller, R.; Brenner, D. Liver fibrosis. *J. Clin. Invest.* **2005**, *115*, 209–218, doi:10.1172/JCI200524282.The.
  31. Friedman, S.L.; Arthur, M.J. Activation of cultured rat hepatic lipocytes by Kupffer cell conditioned medium. Direct enhancement of matrix synthesis and stimulation of cell proliferation via induction of platelet-derived growth factor receptors. *J. Clin. Invest.* **1989**, *84*, 1780–1785.
-

32. Mazza, G.; Al-Akkad, W.; Rombouts, K. Engineering in vitro models of hepatofibrogenesis. *Adv. Drug Deliv. Rev.* **2017**, *121*, 147–157, doi:10.1016/j.addr.2017.05.018.
  33. van Grunsven, L.A. 3D in vitro models of liver fibrosis. *Adv. Drug Deliv. Rev.* **2017**, *121*, 133–146, doi:10.1016/j.addr.2017.07.004.
  34. Rombouts, K. Hepatic stellate cell culture models. In *Stellate Cells in Health and Disease*; Elsevier, 2015; pp. 15–27.
  35. Imai, K.; Sato, T.; Senoo, H. Adhesion between cells and extracellular matrix with special reference to hepatic stellate cell adhesion to three-dimensional collagen fibers. *Cell Struct. Funct.* **2000**, *25*, 329–336.
  36. Evenou, F.; Hamon, M.; Fujii, T.; Takeuchi, S.; Sakai, Y. Gas-permeable membranes and co-culture with fibroblasts enable high-density hepatocyte culture as multilayered liver tissues. *Biotechnol. Prog.* **2011**, *27*, 1146–1153.
  37. Xiao, W.; Kodama, M.; Komori, K.; Sakai, Y. Oxygen-permeable membrane-based direct oxygenation remarkably enhances functions and gene expressions of rat hepatocytes in both 3D and sandwich cultures. *Biochem. Eng. J.* **2014**, *91*, 99–109, doi:10.1016/j.bej.2014.08.005.
  38. Xiao, W.; Shinohara, M.; Komori, K.; Sakai, Y.; Matsui, H.; Osada, T. The importance of physiological oxygen concentrations in the sandwich cultures of rat hepatocytes on gas-permeable membranes. *Biotechnol. Prog.* **2014**, *30*, 1401–1410, doi:10.1002/btpr.1954.
  39. Matsui, H.; Osada, T.; Moroshita, Y.; Sekijima, M.; Fujii, T.; Takeuchi, S.; Sakai, Y. Rapid and enhanced repolarization in sandwich-cultured hepatocytes on an oxygen-permeable membrane. *Biochem. Eng. J.* **2010**, *52*, 255–262.
  40. Nahmias, Y.; Casali, M.; Barbe, L.; Berthiaume, F.; Yarmush, M.L. Liver endothelial cells promote LDL-R expression and the uptake of HCV-like particles in primary rat and human hepatocytes. *Hepatology* **2006**, *43*, 257–265.
  41. Bhatia, S.N.; Yarmush, M.L.; Toner, M. Controlling cell interactions by micropatterning in co-cultures: Hepatocytes and 3T3 fibroblasts. *J. Biomed. Mater. Res. Off. J. Soc. Biomater. Jpn. Soc. Biomater.* **1997**, *34*, 189–199.
  42. Lu, H.-F.; Chua, K.-N.; Zhang, P.-C.; Lim, W.-S.; Ramakrishna, S.; Leong, K.W.; Mao, H.-Q. Three-dimensional co-culture of rat hepatocyte spheroids and NIH/3T3 fibroblasts enhances hepatocyte functional maintenance. *Acta Biomater.* **2005**, *1*, 399–410.
  43. Mesnil, M.; Fraslin, J.-M.; Piccoli, C.; Yamasaki, H.; Guguen-Guillouzo, C. Cell contact but not junctional communication (dye coupling) with biliary epithelial cells is required for hepatocytes to maintain differentiated functions. *Exp. Cell Res.* **1987**, *173*, 524–533.
  44. Ishihara, K.; Mizumoto, H.; Nakazawa, K.; Kajiwara, T.; Funatsu, K. Formation of a sheet-shaped organoid using rat primary hepatocytes for long-term maintenance of liver-specific functions. *Int. J. Artif. Organs* **2006**, *29*, 318–328.
  45. Auth, M.K.H.; Okamoto, M.; Ishida, Y.; Keogh, A.; Auth, S.H.G.; Gerlach, J.; Encke, A.; McMaster, P.; Strain, A.J. Maintained function of primary human hepatocytes by cellular interactions in coculture: implications for liver support systems. *Transpl. Int.* **1998**, *11*, S439–S443.
  46. Guo, R.; Xu, X.; Lu, Y.; Xie, X. Physiological oxygen tension reduces hepatocyte dedifferentiation in in vitro culture. *Sci. Rep.* **2017**, *7*, 1–9.
-



47. Scheidecker, B.; Shinohara, M.; Sugimoto, M.; Danoy, M.; Nishikawa, M.; Sakai, Y. Induction of in vitro Metabolic Zonation in Primary Hepatocytes Requires Both Near-Physiological Oxygen Concentration and Flux. *Front. Bioeng. Biotechnol.* **2020**, *8*, 524.
  48. Haque, A.; Gheibi, P.; Gao, Y.; Foster, E.; Son, K.J.; You, J.; Stybayeva, G.; Patel, D.; Revzin, A. Cell biology is different in small volumes: endogenous signals shape phenotype of primary hepatocytes cultured in microfluidic channels. *Sci. Rep.* **2016**, *6*, 33980.
  49. Tsuchida, T.; Friedman, S.L. Mechanisms of hepatic stellate cell activation. *Nat. Rev. Gastroenterol. Hepatol.* **2017**, *14*, 397–411, doi:10.1038/nrgastro.2017.38.
  50. Koyama, Y.; Brenner, D.A. Liver inflammation and fibrosis. *J. Clin. Invest.* **2017**, *127*, 55–64.
  51. Hellerbrand, C.; Stefanovic, B.; Giordano, F.; Burchardt, E.R.; Brenner, D.A. The role of TGF $\beta$ 1 in initiating hepatic stellate cell activation in vivo. *J. Hepatol.* **1999**, *30*, 77–87.
  52. Breitkopf, K.; Godoy, P.; Ciucan, L.; Singer, M. V; Dooley, S. TGF- $\beta$ /Smad signaling in the injured liver. *Z. Für Gastroenterol.* **2006**, *44*, 57–66.
  53. Friedman, S.L. Hepatic stellate cells: protean, multifunctional, and enigmatic cells of the liver. *Physiol. Rev.* **2008**, *88*, 125–172.
  54. Thiele, N.D.; Wirth, J.W.; Steins, D.; Koop, A.C.; Ittrich, H.; Lohse, A.W.; Kluwe, J. TIMP-1 is upregulated, but not essential in hepatic fibrogenesis and carcinogenesis in mice. *Sci. Rep.* **2017**, *7*, 714, doi:10.1038/s41598-017-00671-1.
  55. Hemmann, S.; Graf, J.; Roderfeld, M.; Roeb, E. Expression of MMPs and TIMPs in liver fibrosis - a systematic review with special emphasis on anti-fibrotic strategies. *J. Hepatol.* **2007**, *46*, 955–975, doi:10.1016/j.jhep.2007.02.003.
  56. Arpino, V.; Brock, M.; Gill, S.E. The role of TIMPs in regulation of extracellular matrix proteolysis. *Matrix Biol.* **2015**, *44–46*, 247–254, doi:10.1016/j.matbio.2015.03.005.
  57. Yoshiji, H.; Kuriyama, S.; Miyamoto, Y.; Thorgeirsson, U.P.; Gomez, D.E.; Kawata, M.; Yoshii, J.; Ikenaka, Y.; Noguchi, R.; Tsujinoue, H.; et al. Tissue inhibitor of metalloproteinases-1 promotes liver fibrosis development in a transgenic mouse model. *Hepatology* **2000**, *32*, 1248–1254, doi:10.1053/jhep.2000.20521.
  58. Hernandez-Gea, V.; Friedman, S.L. Pathogenesis of Liver Fibrosis. *Annu. Rev. Pathol. Mech. Dis.* **2011**, *6*, 425–456, doi:10.1146/annurev-pathol-011110-130246.
  59. Bhatia, S.N.; Underhill, G.H.; Zaret, K.S.; Fox, I.J. STATE OF THE ART REVIEW Cell and tissue engineering for liver disease. **2014**, *6*.
  60. Vanhaecke, T.; Rogiers, V. Hepatocyte cultures in drug metabolism and toxicological research and testing. In *Cytochrome P450 Protocols*; Springer, 2006; pp. 209–227.
  61. Walker, T.M.; Rhodes, P.C.; Westmoreland, C. The differential cytotoxicity of methotrexate in rat hepatocyte monolayer and spheroid cultures. *Toxicol. In Vitro* **2000**, *14*, 475–485.
  62. Curcio, E.; Salerno, S.; Barbieri, G.; De Bartolo, L.; Drioli, E.; Bader, A. Mass transfer and metabolic reactions in hepatocyte spheroids cultured in rotating wall gas-permeable membrane system. *Biomaterials* **2007**, *28*, 5487–5497.
-